Analysis of human physical vulnerability using static equilibrium techniques of a Hazard flood for the determination of unsafe areas in the city of Catacaos – Piura, Peru

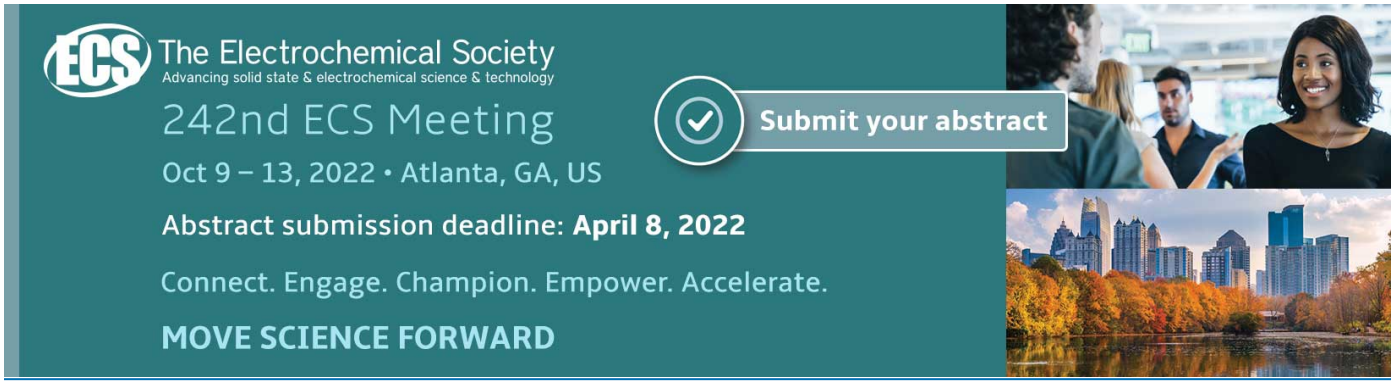

Analysis of human physical vulnerability using static equilibrium techniques of a Hazard flood for the determination of unsafe areas in the city of Catacaos – Piura, Peru

J A Carrizales[1], M C Rodas[1] and L F Castillo[2]

[1]Bachelor, Peruvian University of Applied Sciences, Lima - Peru
[2]Magister Scientiae, Peruvian University of Applied Sciences, Lima – Peru

E-mail: [1]u201519101@upc.edu.pe ; [2]u201522774@upc.edu.pe ; [3]pccilcas@upc.edu.pe

Abstract. Heavy rains and El Niño phenomenon are recurring natural phenomena at a national level. These can cause floods due to the overflowing of rivers, which, when close to cities, can cause both human and material losses. The district of Catacaos, located in the city of Piura, was the one with the highest number of injuries due to the flood caused by El Niño phenomenon in 2017. This phenomenon causes a large amounts of rainfalls due to the presence of abnormally warm waters along the northern coast of Peru [1]. It is for this reason that the need arose to carry out an analysis of the physical vulnerability due to instability of people through static equilibrium, in said district, in order to present maps of unsafe areas in the face of this phenomenon. In this investigation, flood hazard maps are generated simulating the one presented in 2017, using 2D hydraulic modeling. For the generation of vulnerability curves, the instability analysis is performed by moment and drag force. Finally, maps with unsafe areas are made using ArcGis software. Where the results obtained indicate that 29.37% of the city was flooded. Likewise, the vulnerability maps generated show us that women and men over 18 years of age in the city of Catacaos would be vulnerable to dragging and overturning in the face of floods in 16.54% and 13.21%, respectively, of the total studied area. This information will be useful for the development of future evacuation plans during floods, carried out by national entities.

Keywords: Hazard flood, people instability, vulnerability curves, static equilibrium

1. Introduction

The definition of the word flood is presented as the “overflow of water outside the normal limit of a river or any body of water” [2]. This type of disaster is the one that generates the largest number of affected people worldwide. [3]. Peru presents a large number of floods each year due to heavy rains and the El Niño Costero phenomenon. In 2017, the El Niño Costero phenomenon caused great material damage and many victims. The department of Piura registered 30,973 flood victims, being one of the most affected cities by this phenomenon. [4]. Similarly, the Catacaos district, belonging to the city of Piura, was the one that presented the highest number of injured. For this reason, it is necessary to carry out the modeling of instability hazard maps of people in the event of a flood. This type of mapping will help to carry out flood prevention programs and to locate areas where water levels and speed are reached to a point where they can cause both material and human damages.

For the modeling of flood maps, computer programs such as Hydrologic Engineering Center and River Analysis System (HecRas) or Geo HecRas are frequently used in conjunction with ArcGis software. Factors such as flood exposure, flood damage, and flood characteristics can be used to create flood hazard maps [5]. Besides that, some studies use information on topography, rainfall values, Manning coefficient values and sediment granulometry. [6].

On the other hand, there are different ways of analyzing the instability of people in a flow, in[7] instability is analyzed through laboratory tests using real people, while in [8] was analyzed taking into account the forces acting on the body, separating them into dynamic and static actions to identify groups of variables. Finally, in [9] the instability of the person is related to the instability due to overturning and sliding.

2. Methodology

2.1. Area of study.

The purpose of the research is to provide flood hazard and people vulnerability maps for the city of Catacaos, which has frequent flooding. The area of study is located in the department of Piura. Geographically it is located at the coordinates 5° 15'42" of south latitude and 80° 40'27" of west longitude. To the north, it borders the districts Veintiseis de Octubre, Piura and Castilla. To the east and south, it borders the Lambayeque province of the Lambayeque department.

According to the census conducted in 2017 by the National Institute of Statistics and Informatics (INEI), Catacaos had 75,870 inhabitants, of which 97% live in urban areas and 3% in rural areas.

Among the city's economic activities are agriculture, commerce, handicrafts, fishing, mining, etc. According to information compiled by INEI, in 2015, the percentage of the population engaged in agriculture represents 27.9%.

In addition, the report [10] shows that, up until 2017, 5 types of private dwellings were identified in the district: independent house, apartment in a building, tenement house, improvised dwelling, and premises not intended for human habitation. A total of 18,280 dwellings were surveyed, with a predominance of independent houses.

2.2. Characterization of the study site.

The city of Catacaos is located within the Piura basin. It has a total area of 10,930.110 km^2 and a perimeter of 652.307 km. The section of the studied river is approximately 2,600 m long, with an average channel slope of 0.08% and an average width of 140 m. The area of study belonging to the city of Catacaos has a total surface area of 681 ha. All these data were obtained through RPAS images provided by the National Center for the Estimation, Prevention and Reduction of Disaster Risk (CENEPRED) in collaboration with the Information System for Disaster Risk Management (SIGRID). The obtained information included an orthomosaic of 2728 photos, a spatial resolution of 5.14 cm and a flight area of 1649.33 ha, contour lines with an interval at every 1 meter, a Digital Surface Model (DSM) and a Digital Terrain Model (DTM), both in .sid format. This data record was conducted in 2019 and from this information only 736.74 ha were carried out as shown in figure 1.

Figure 1. RPAS images of the studied area.

2.3. Characteristic data of the population

For the application of the formulas presented in the vulnerability analysis, the data of weight and average height of the inhabitants of the Catacaos area will be used. According to a study presented in 2018 at the annual meeting of the Society for Genomic Biology at Harvard, it was found that the average height of Peruvian men over 18 years is 1.65 m and of Peruvian women 1.52 m [11]. Similarly, the publication [12] made by the National Institute of Statistics and Informatics (INEI) shows that 38.9% of the coastal population over 15 years of age is overweight, with an average Body Mass Index (BMI) of 26.2. Thus, the following characteristic data to be used were obtained as shown in table 1:

Table 1. Values of height, body mass index (BMI) and weight for Peruvian men and women with overweight.

Genre	Height [m]	Weight [kg]	BMI
Male	1.65	71.3	26.2
Female	1.52	60.5	26.2

2.4. Vulnerability Analysis.

The physical stability of a person in the water may depend on different factors depending on the approach required. S.N. Jonkman and E. Penning-Rowsell in [9] focus on the analysis of the hydrodynamic mechanisms acting on the body, which are overturning instability and dragging instability. The first occurs when the moment generated by the weight of the body is less than the moment caused by the force of the fluid during a flood upon the human body.

Moment generated by drag

$$M_{drag} = h \times 0.5 \times C_d \times B \times \rho_w \times h \times v^2$$

Moment generated by weight

$$M_{weight} = m \times g \times L \times cos\ (\alpha)$$

Condition of instability by toppling

$$M_{drag} > M_{weight}$$

On the other hand, the instability due to drag force is caused when the friction force between the person's feet and the ground is less than the horizontal force generated by the fluid upon said body.

Friction force

$$F_{friction} = \mu \times m \times g$$

Drag force

$$F_{drag} = 0.5 \times \rho_w \times C_D \times B \times h \times v^2$$

Instability by drag condition

$$F_{drag} > F_{friction}$$

Where ρ is the density of the fluid, C_D the drag coefficient, B the width of the human body, μ the friction coefficient, m the mass of the body, L the height of the body, h the depth of flow, and v the fluid speed.

On the other hand, previously conducted studies suggest using an average human body width of 0.4 m and a drag coefficient of 1.1 in the case of the human body. Also, it is suggested to analyze the vulnerability taking into account a maximum flow speed of 3 m/s. For our research we used a friction coefficient of 0.5, an inclination angle of 70 degrees, and a water density of 1500 kg /m^3. These data may vary depending on the analysis to be performed.

2.5. Frequency analysis.

In the frequency analysis, the data obtained by the Sanchez Cerro hydrometric station was considered. In addition, as shown in figure 2, the Hydrological Frequency Analysis (Hyfran) program was used to obtain the description of the total flows, where a total of 48 maximum instantaneous flows, the standard deviation, median, and the maximum and minimum of the previously specified data can be seen.

The next step was to adjust the behavior of the data obtained from the station to a theoretical probability distribution. The used methods were: Exponential method, Gumbel, Weibull, Gamma and Log-Pearson Type III. To choose the most suitable for the frequency analysis, the graphical method, the verification by the Chi-square test and the criteria of comparison of distributions were used.

With the graphical method, it was possible to observe the probabilistic method that best behaves with our data. A 95% confidence interval was presented.

Through the Chi-square test, the Hyfran program determines whether the method should be accepted with a significance level of 5%. In this way, the Gumbel method was discarded.

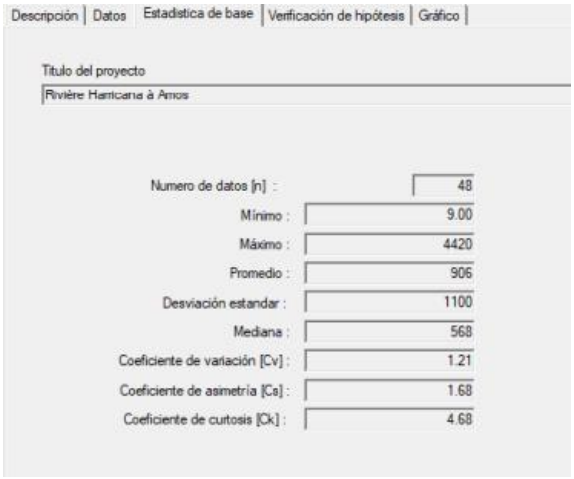

Figure 2. Description of the total of maximum flow rates.

Finally, with the distribution comparison criteria, the method with the lowest Akaike Information Criterion (AIC) and Bayesian Information Criterion (BIC) was chosen, having the return periods (period of time in which an event will be equaled or surpassed in magnitude, at least once) as a working group of 50, 100 and 200 years.

It was observed that the probabilistic method that presented the lowest AIC and BIC was Gamma. Therefore, as it was also accepted in the graphical method and by the Chi-square test, the flows obtained by it were used.

2.6. Design flows for different periods.

The design flows for the return periods of 25, 50, 100, 200 and 500 years were calculated using the Gamma method. In this way, the return period was determined with the flow that most closely resembled the one presented in 2017, which was 3,468m^3/s [13].

The flows found for each return period are those presented in table 2.

Table 2. Flows found by return period.

Return period [years]	Flow [m^3/s]
25	3450.00
50	4330.00
100	5220.00
200	6120.00
500	7330.00

This way, the return period of 25 years was chosen for practical purposes, being the closest to the period presented in 2017. Thus, the return period used for modeling the flood maps will be 25 years.

2.7. Modelling methodology

2.7.1. Topography. The topographic survey obtained from the SIGRID web page, whose corporate author is CENEPRED, was first used to create the flood hazard maps. As mentioned above, the contour lines are spaced every 1 meter and were obtained from drone photography.

The ArcGis program was used to transform the contour lines to Digital Elevation Model (DEM), Tagged Image File Format (TIFF), and Triangle Irregular Network (TIN) files, in such a way that it can be exported to the Hec-Ras program. And finally, these DEM and TIN files will be used in the Hec-Ras program to carry out all the modeling of the place with the help of RAS Mapper.

2.7.2. Manning. The value of Manning's number for the channel that was considered was the one found in [14], being 0.030. In addition, n1 was considered equal to 0.016 for the area with land for agricultural use, and n3 equal to 0.011 for the urban area; these values are shown in table 3. The zoning of Manning's number according to the land use of the work area was carried out with the help of the shapefile obtained from the Ministry of Environment (MINAM) in its digital coverage map. Which represents through polygons the agricultural areas, rivers and urban areas.

Table 3. Manning values used.

N1	N2	N3
0.016	0.030	0.011

2.7.3. Modelling with HecRas 2D.

2.7.3.1. Netting and refinement. Using the topography obtained in ArcGis, the DEM of the study area was placed as terrein in the HecRas program. Using this map, the area was netted with a 10x10m grid. After that, the river channel area was refined using a 5x5 m net to improve the iterations carried out by the program and to obtain better results. It is important to mention that as the width of the net is reduced, the modeling will be much more accurate, but the processing time will increase.

2.7.3.2. Boundary conditions. To finish the modeling, we proceeded to place outline conditions that will allow us to place the entry hydrograph and the exit point of the runoff. The inflow hydrograph will be placed upstream while the runoff point will be placed downstream. The hydrograph mentioned in point 2.5 was used, which belongs to the return period of 25 years and the slope used downstream will average 0.08%.

2.7.4. Modelling with ArcGis. Once the results of the Hec-Ras program were obtained, we proceeded to export the shapes of the depths and speeds in the time that best represented the flood occurred in 2017 (explained in the calibration process). After that, a sampling net with 5x5 meter pixels was carried out over the study area, since the shapes obtained from the Hec-Ras were conducted with a net of the same dimension. The importance of this point is to cover the entirety of the pixels obtained in the modeling of the hazard maps.

After carrying out the netting, the Spatial Join command was used to copy the properties of the shapes of depths and speeds in the net already made. This allowed us to obtain 5x5 squares with their corresponding depths and speeds values.

The aforementioned was necessary, since a single table is needed to work the data with the instability formulas, both by turning and by force. Within the table we proceeded to add rows and place the moment and force values generated by the weight, using the characteristic data of the population, as these are not speed or depth dependent. Subsequently, with the help of the Field Calculator command, the formulas for both overturning instability and dragging were placed by pulling the values of speed and depth from the same table.

With the help of the same command "Field Calculator", a conditional was placed inside the table, where the program was asked that if the value of the force generated by friction was less than the drag force (already determined and placed previously) then it would place unstable, while if the aforementioned did not happen, it would place stable. The same was carried out for the case of the moment, if the moment generated by the weight was less than the moment generated by the drag force, then it had to place instability and vice versa.

Conditional for drag instability

If [F_{drag}]> [$F_{Friction}$] then
a="unstable"
end if

If [F_{drag}]<[$F_{Friction}$] then
a="stable"
end if

Conditional for toppling instability

If [M_{weight}] > [M_{drag}] then
a="stable"
end if

If [M_{weight}] < [M_{drag}] then
a="unstable"
end if

Finally, in order to obtain a vulnerability map that represents both the instability by toppling and dragging in a single shape, the instability tables of both cases were joined through the Joins and Relates command. By means of this command, the tables of both maps already determined were all in one, and to join these conditions the Field Calculator was used for the last time. Here we ask the program to place unstable in cases where there is instability due to overturning and sliding. In the same way, if there was stability for both cases to be placed stable and if there was instability in one case and stability in the other, the instability should be considered, since the person presented a possibility of showing damage in that area of 25m^2.

If [Condition Force] <> [Condition Moment] then
a="unstable"
end if

If [Condition Force] ="unstable" and [Condition Moment] = "unstable"
then
a="unstable"
end if

If [Condition Force] ="stable" and [Condition Moment] = "stable"
then
a="stable"
end if

The complete process mentioned before is summarized in the flow chart shown in figure 3.

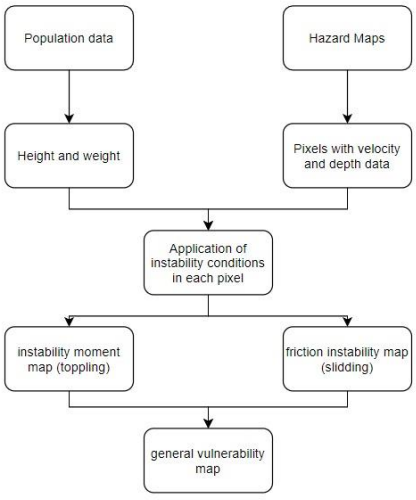

Figure 3. Methodology flow chart for modeling with ArcGis.

3. Results and calibration

3.1. Calibration process

In order to validate our flood areas, we had to compare the area with records of the 2017 flood caused by the El Niño phenomenon. Similarly, a visit was made to the city of Catacaos to collect testimonies from the inhabitants about the extent of the flooding and approximately how high the water flow reached with respect to the ground. Thus, when determining the flood areas, multiple processing was carried out by continuously changing the Manning's number until the flood area represents what happened in the 2017 event. The validation flowchart used is shown in figure 4.

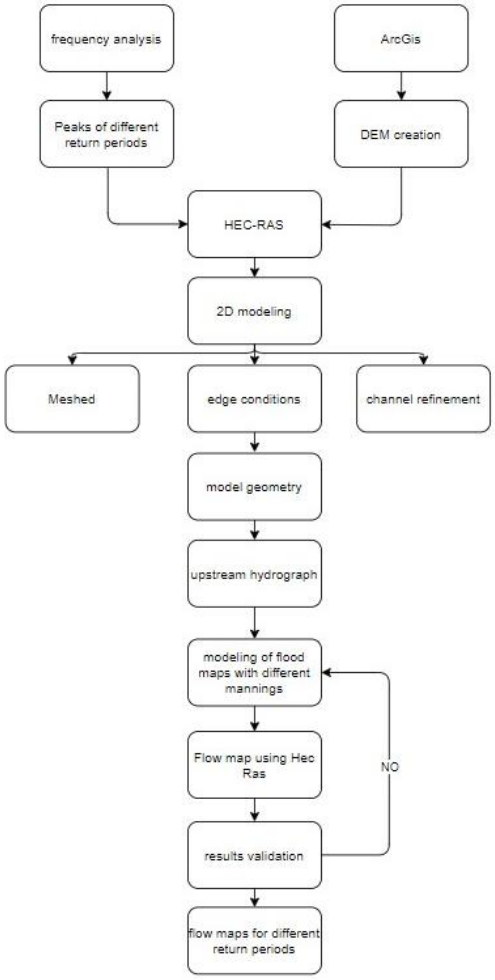

Figure 4. Validation flowchart for the realization of the flood map.

3.2. Results of depth values

The map of depth values for a flood obtained by the HecRas program is shown in figure 5. This map was modeled in 2D with a time interval of 1 min for the 3 days of the histogram representing only the maximum point of this, which is a flow of 3450 m^3/s, representative flow rate for the year 2017. The water depth values presented vary from 0 to 15 m.

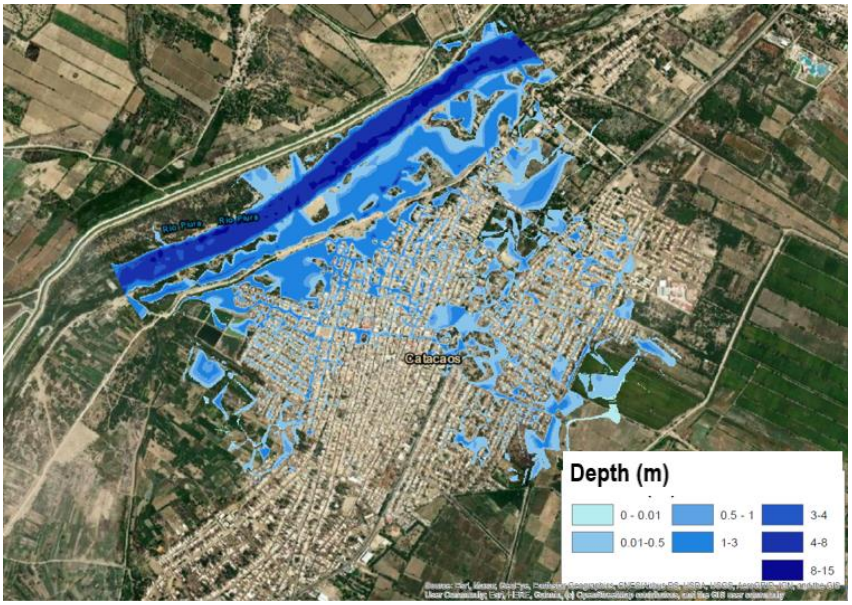

Figure 5. Map of depth values (m) for a flood with a flow of 3450 m^3/s

As it can be seen in figure 5, in the urban area of the city and its plain, the maximum depth value was 3 m.

3.3. Results of velocities.

Similarly, the velocity map in figure 6, was made for the return period of 25 years (with representative flow for 2017). The velocity range is from 0 to 20 m/s.

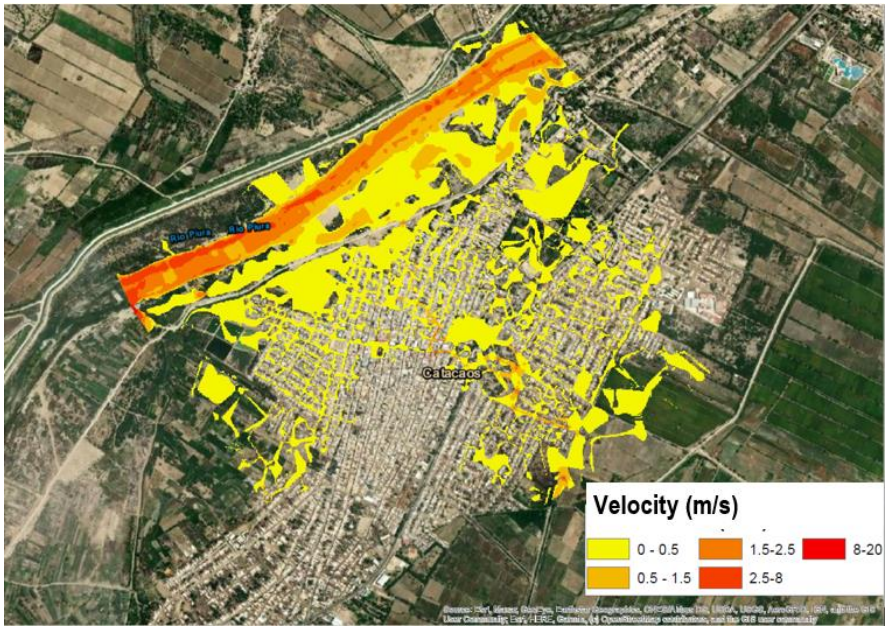

Figure 6. Map of velocity values (m/s) for a flood with a flow of 3450 m^3/s.

According to the flood maps obtained with Hec-Ras, the velocity values inside the riverbed vary between 8 and 20 m/s, while velocities within urban area of the city vary from 0 to 2.5 m/s. On the other hand, velocities in the city plain vary from 0 and 1.5 m/s.

3.4. Results of vulnerability maps.

In the maps shown in Figures 7 and 8, can be appreciated the contrast between the flooded area, represented by color blue, and the area of vulnerability, represented by color red, for women and men over the age of 18 years.

According to the maps obtained, it was observed that the area of vulnerability due to the effect of the moment and force of drag in women was 31.87 Ha, which would be 16.54% of the flooded area; and that the area of vulnerability due to the effect of the moment and drag force in men was 25.45 Ha, which would be 13.21% of the flooded area.

It was appreciated that the area of vulnerability due to the effect of the moment and force of drag in women would be notably bigger than the area of vulnerability in men.

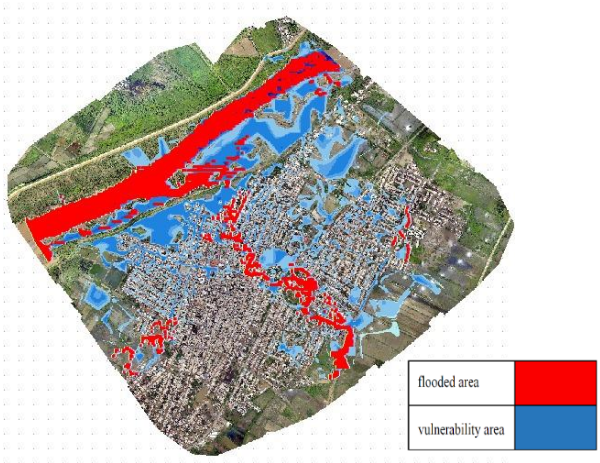

Figure 7. Instability vulnerability map by moment and friction force for women.

Figure 8. Instability vulnerability map by moment and friction force for men.

Finally, it is important to point out the areas where the inhabitants would present high vulnerability during a flood. The most notable areas were:

- The surroundings of the populated center “Pueblo Nuevo”, more specifically the Comercio, Cepita, San Francisco, Piura and Chota streets.
- Tumbes, Cusco and Calletano Heredia streets closely to the Manuel O.Feijo stadium.
- Surroundings and interiors of human settlement San Juan Bautista.
- The city plain surrounded by Calle 1, Calle 2 streets and Los Sechuras avenue.

3.5. Analysis and generation of vulnerability curves.

Using the characteristic data of the population and the formulas mentioned in the vulnerability analysis, curves shown in Figures 9 and 10, were obtained that represent the stability of the Catacaos population before a flow. The area designated as "stable" is limited at the top by the intersection of the curves of instability by moment and instability by force of drag. In the case of men, the intersection is given for a depth of 1.12 m and a velocity of 0.97 m/s, and for women it is given for a depth of 1.03 m and a velocity of 0.93 m/s.

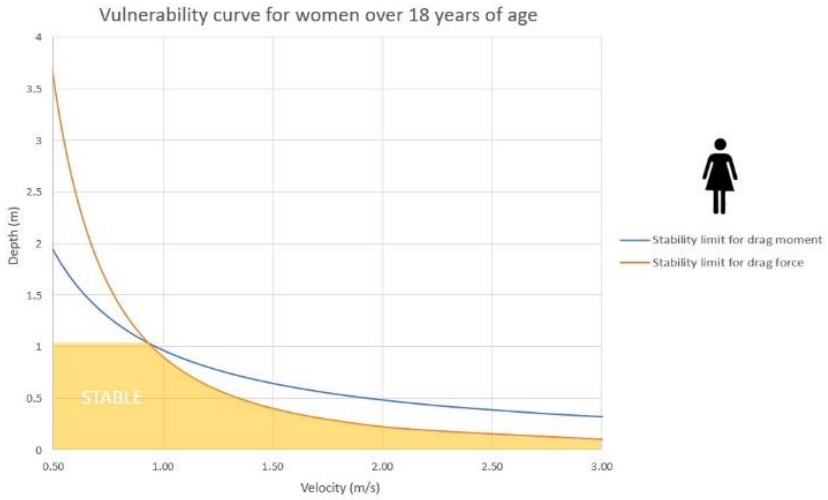

Figure 9. Vulnerability curves for instability by moment and force for women.

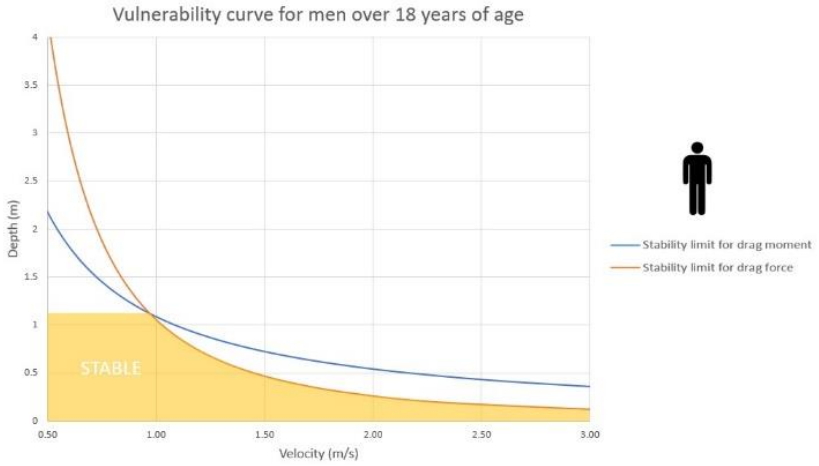

Figure 10. Vulnerability curves for instability by moment and force for men.

4. Conclusions

- The total flooded area found was 192.70 Ha, which represents 29.37% of the total area studied.
- The maximum depths obtained in the 2017 event were within the channel, with depth values that vary between 4 and 15 m. While the depth values obtained within the urban area of the city, go from 0.5 to 3 meters of height.
- Velocities obtained within the urban area of the city, for the period of return of 25 years, vary from 0 to 1.5 m/s.
- The area corresponding to vulnerability due to floods for men over 18 years of age is included in the vulnerability map for women, since women present less height and weight than men.
- Vulnerability is determined by the two instability conditions and the forces mentioned. Calculations may be improved analysing other interacting forces such as buoyancy and lift.
- The maps obtained can be used by different entities, that are in charge of the decision making in cases of flooding, to determine unsafe areas in order to prepare mitigation and emergency plans.

5. Recommendations

- It is recommended to carry out your own topographic survey with drones, since the downloadable data from the different institutions may present errors, which reduces the precision of the results.
- A visit to the study site is always recommended, as this allows to validate the topography data and the Manning coefficient values used for modelling.
- It is important to mention that the more detailed the topography is, the greater the precision of the results in modelling flow or hazard maps.
- It is recommended to validate the flow map modelling, using other programs such as IBER and Flo2D.

References

[1] Instituto Geofísico del Perú 2017 *Generación de información y monitoreo del Fenómeno El Niño*
[2] UNESCO-WMO 2013 *International Glossary of Hydrology* (UNESCO)
[3] Oficinas de Naciones Unidas Para la Reducción del Riesgo de Desastres, UNDRR 2019 Available: https://eird.org/americas/noticias/2018-60-millones-de-personas-resultaron-afectadas-por-diversos-eventos-meteorologicos-extremos.html#.X1VlgchKjIV
[4] World Metereological Organization, Atlas of Mortality and Economic Losses from, World Metereogical Organization, 2014.
[5] DesInventar Sendai, Sendai Framework For Disaster Risk Reduction, Available: https://www.desinventar.net/DesInventar/country_profile.jsp?countrycode=per&lang=ES.
[6] Organización Mundial de la Salud, Organización Panamericana de la Salud 2017 Lluvias e Inundaciones en Perú, Centro de Operaciones de Emergencia de la Organización Panamericana de la Salud
[7] Xia J, Guo P, Zhou M, Falconer R, Wang Z and Chen Q 2018 Modeling of flood risks to people and property in flood diversion zone *J. Zhejiang University-Science A* **19** 864–77
[8] Arrigui C, Oumeraci H y Castelli F 2017 Hydrodynamics of pedestrians' instability in floodwaters *Hydrol. Earth Syst. Sci.* **21** 515–31
[9] Jonkman S N and Penning-Rowsell E 2018 Human Instability in Flood Flows *J. Am. Water Resour. Assoc.* **44** 1-11
[10] Instituto Nacional de Estadística e informática 2018 *Perú: Características de las viviendas particulares y los hogares* (Peru: Lima)
[11] RPP Noticias 2018 Los peruanos tienen una de las tallas más bajas del mundo (Peru: Lima)
[12] Instituto Nacional de Estadistica e Informatica 2016 Available: https://www.inei.gob.pe/prensa/noticias/el-355-de-la-poblacion-peruana-de-15-y-mas-anos-de-edad-padece-de-sobrepeso-9161/
[13] Estado Situacional de la Emergencia 2017 Available: http://sinpad.indeci.gob.pe/sinpad/emergencias/Evaluacion/Reporte/rpt_eme_situacion_emergencia.asp?EmergCode=00084822
[14] Maza-Sócola J 2019 Análisis del comportamiento hidráulico del río Piura, en el tramo Los Ejidos-Puente Independencia Piura